

The Effect of Low-Temperature Heat Treatment on the Magnetic Properties of Biogenic Ferrihydrite Nanoparticles

D. A. Balaev^{a, b*}, A. A. Krasikov^b, A. A. Dubrovskii^a, O. A. Bayukov^a,
S. V. Stolyar^{a, b}, R. S. Iskhakov^a, V. P. Ladygina^c, and R. N. Yaroslavtsev^b

^a Kirensky Institute of Physics, Siberian Branch, Russian Academy of Sciences, Krasnoyarsk, 660036 Russia

^b Siberian Federal University, Krasnoyarsk, 660041 Russia

^c Krasnoyarsk Scientific Center, Siberian Branch, Russian Academy of Sciences, Krasnoyarsk, 660036 Russia

*e-mail: dabalaev@iph.krasn.ru

Received February 13, 2015

Abstract—We have studied the influence of low-temperature heat treatment (annealing) on the magnetic properties of superparamagnetic nanoparticles of biogenic ferrihydrite. It is established that the proposed treatment leads to an increase in the blocking temperature and magnetic susceptibility of samples. After subsequent exposure in aqueous medium, the magnetic properties of annealed sol remain constant. The character of changes in the magnetic properties of samples studied shows that low-temperature heat treatment allows nanoparticle dimensions to be increased in a controlled way.

DOI: 10.1134/S1063785015070172

The known variety of magnetic nanoparticles includes a class of biogenic ones that are produced as a result of the living activity of organisms and bacteria. The best-known and most exhaustively studied of these is ferritin [1–4], which is a ferrihydrite situated inside a protein shell. Ferrihydrite exhibits an antiferromagnetic (AF) order, but a defect structure and small sizes of ferrihydrite particles (~5–8 nm) [4, 5] allow them to possess an uncompensated magnetic moment μ_{unc} reaching several hundred Bohr magnetons, which results in a characteristic superparamagnetic (SP) behavior of ferrihydrite nanoparticles. This circumstance makes it possible to use ferrihydrite nanoparticles in practice, e.g., as carriers of drugs in an organism.

Our previous investigations [5–7] showed that the properties of nanosized ferrihydrite particles produced as a result of the vital activity of *Klebsiella oxytoca* bacteria are similar to those of ferritin, which is manifested by the existence of μ_{unc} , SP behavior, blocking temperature (T_B), and magnetization hysteresis at $T < T_B$. It was also found [7] that heat treatment (annealing) of the initial sol of ferrihydrite particles for 3 h at a relatively low temperature (within 140–1500°C) leads to a twofold increase in T_B . Based on the classical relation

$$kT_B = kV/\ln(\tau/\tau_0) \approx KV/25 \quad (1)$$

(where K is the magnetic anisotropy constant; V is the particle volume; and $\tau \sim 10^2$ and $\tau_0 \sim 10^{-9}$ – 10^{-10} s are the characteristic times of measurement and particle relaxation, respectively) and an analysis of magnetiza-

tion curves $M(H)$ measured at $T > T_B$, it was established that the annealing led to coarsening of the ferrihydrite particles.

The present work was aimed at (i) studying the dependence of the blocking temperature of ferrihydrite on the duration of its low-temperature heat treatment (increased up to 240 h) and (ii) elucidating the possible effect of subsequent hydration of the annealed ferrihydrite on its blocking temperature.

Ferrihydrite nanoparticles in the sol form were prepared as described previously [8, 9]. The samples were additionally heat treated in air at 150°C for various times, and it was found that the sol loses up to 25 mass % (upon annealing for 240 h). This is evidently related to the loss of water, since this is admitted by the nominal formula $\text{Fe}_2\text{O}_3 \cdot 9\text{H}_2\text{O}$. In what follows, these samples will be denoted as FH- X , where X is the total annealing time (in hours). After annealing, some samples were exposed for 3 days in saturated water vapor at room temperature, which led to a 15–20% increase in the sample mass (these samples are denoted as FH- X -H).

The Mössbauer spectra were measured at room temperature on an MC-1104Em spectrometer with a $^{57}\text{Co}(\text{Cr})$ source. The magnetic properties were studied using a vibrating-sample magnetometer. The temperature dependences of the magnetic moment $M(T)$ were measured in the regimes of cooling without an applied field (zero-field cooling, ZFC) and an external field of $H = 1$ kOe (field cooling, FC). Temperature dependence $M(T)$ measured at $H = 1$ kOe was recalculated to magnetic susceptibility $\chi(T) = M(T)/H$.

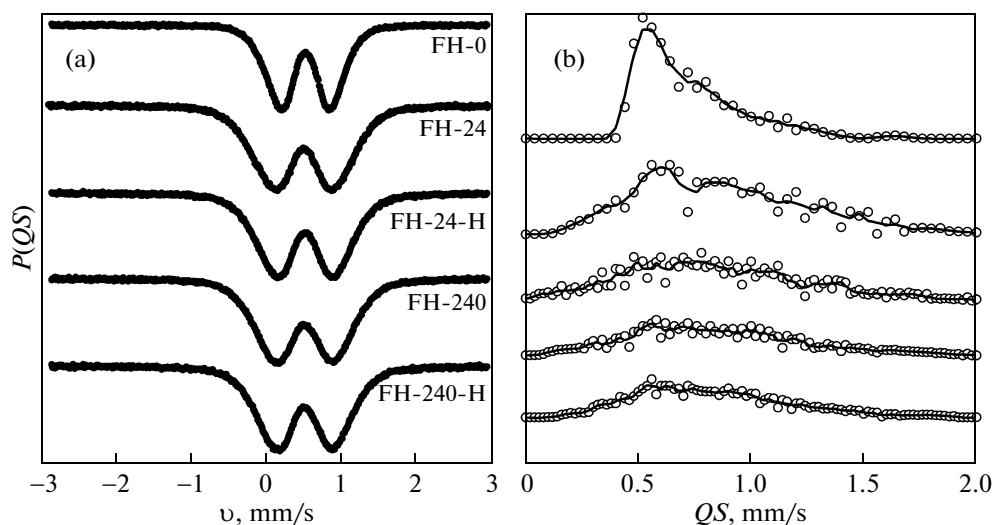


Fig. 1. (a) Room-temperature Mössbauer spectra of annealed and hydrated ferrihydrite samples and (b) the corresponding distributions of quadrupole splitting QS .

The observed Mössbauer spectra represent broadened quadrupole doublets (Fig. 1a) with chemical isomer shifts corresponding to Fe^{3+} cations. Analysis of

the distributions of quadrupole splitting QS (see Fig. 1b and the table) shows evidence of the presence of some nonequivalent Fe positions in ferrihydrite

Mössbauer parameters of ferrihydrite: isomer shift (IS), quadrupole splitting (QS), line width (W), and occupancy of iron positions (A)

Sample	IS (± 0.005 mm/s)	QS (± 0.01 mm/s)	W (± 0.01 mm/s)	A (± 0.03)	Position
FH-0	0.334	0.45	0.24	0.24	Fe1 (cubic)
	0.334	0.69	0.28	0.41	Fe1 (hexagonal)
	0.320	1.00	0.40	0.35	Fe1 (interblock)
FH-24	0.323	0.33	0.28	0.11	
	0.335	0.63	0.33	0.37	Fe1
	0.332	0.95	0.31	0.28	Fe2
	0.325	1.29	0.30	0.16	Fe3
	0.324	1.67	0.33	0.08	
FH-24-H	0.313	0.31	0.30	0.09	
	0.338	0.54	0.28	0.27	Fe1
	0.337	0.80	0.27	0.26	Fe2
	0.332	1.07	0.29	0.23	
	0.327	1.38	0.28	0.11	Fe3
FH-240	0.325	1.75	0.31	0.04	
	0.300	0.25	0.27	0.09	
	0.328	0.55	0.32	0.32	Fe1
	0.328	0.84	0.29	0.28	Fe2
	0.328	1.12	0.27	0.16	
FH-240-H	0.324	1.40	0.27	0.09	Fe3
	0.319	1.74	0.31	0.06	
	0.310	0.35	0.28	0.13	
	0.332	0.63	0.30	0.31	Fe1
	0.327	0.95	0.35	0.37	Fe2
	0.330	1.35	0.41	0.19	Fe3

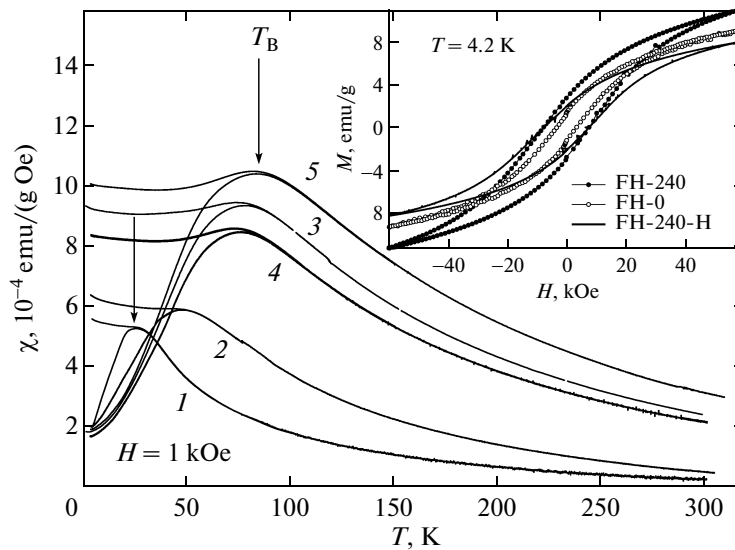


Fig. 2. Plots of $\chi(T)$ measured in ZFC (lower curves) and FC at $H = 1$ kOe (upper curves) regimes for samples (1) FH-0, (2) FH-3, (3) HF-24, (4) FH-24-H, and (5) FH-240 (arrows indicate SP-blocking temperature T_B). The inset shows $M(H)$ curves of some samples measured at $T = 4.2$ K.

samples. In the initial sample (FH-0), there are three Fe positions [10], two of which (Fe1 and Fe2) are attributed to ferrihydrite regions with predominantly cubic and hexagonal packing of ligands, respectively, while the third position (Fe3) is assigned to iron cations occurring in ferrihydrite interlayers.

Low-temperature heat treatment for 24 h (FH-24 sample) leads to a change in the crystallochemical structure of ferrihydrite nanoparticles. The occupancy of Fe1 positions increases at the expense of Fe2 positions with hexagonal packing of ligands. There also appear new positions with lower and higher degrees of distortion of the local environment (partial amorphization of the material), which is manifested by broadening of the $P(QS)$ distribution. The exposure in saturated water vapor (FH-24-H sample) leads to additional amorphization, with further decrease in the number of occupied F1 positions. Amorphization is likely favored by nanometer sizes of ferrihydrite particles. After prolonged annealing (FH-240), the occupancy of main iron positions (Fe1, Fe2, Fe3) in the ferrihydrite structure increases, which is probably related to the formation of coarse particles, as manifested by narrowing of the $P(QS)$ distribution. The subsequent exposure in water vapor (FH-240-H) favors this process, although coarsening is related predominantly to the growth of regions with hexagonal packing of ligands.

Figure 2 shows the temperature dependences of magnetic susceptibility $\chi(T)$ measured in ZFC and FC regimes, which exhibit the characteristic SP behavior. The $\chi(T)_{ZFC}$ curves have maxima in the vicinity of which the behavior differs from that of $\chi(T)_{FC}$. Annealing for 240 h leads to growth in the blocking

temperature (i.e., maximum of the $\chi(T)_{ZFC}$ curve) from ~ 23 to ~ 82 K and to an increase in the magnetic moment at $H = 1$ kOe. At $T < T_B$, the $M(H)$ curves exhibit a hysteresis (see the inset to Fig. 2). The annealed samples possess higher coercivities H_C as compared to that of the initial sample (HF-0). Analogous behavior is observed for the magnetic susceptibility, room-temperature value $\chi(300$ K) of which increases after annealing.

According to the Stoner–Wohlfarth model [11], the coercivity of noninteracting monodomain particles is

$$H_C \approx (K/M_S)[1 - (T/T_B)^{1/2}]$$

where $M_S = \mu_{unc}/V$ is the saturation magnetization. With neglect of a weak variation of the term $[1 - (T/T_B)^{1/2}]$ near $T = 4.2$ K, this formula yields $H_C \sim KV/\mu_{unc}$. Uncompensated magnetic moment μ_{unc} of small AF particles usually obeys the relation $\mu_{unc} \sim V^n$, where n takes a value of either $2/3$ (for an odd number of planes in the case of AF ordering) or $1/2 \leq n \leq 1/3$ (in the presence of defects in the volume or on the surface of particles) [4]; for ferritin and ferrihydrite, n is close to $1/2$ [1, 4, 6, 7]. Therefore, we can more or less assume that $H_C \sim KV^{1/2}$.

The value of susceptibility χ also depends on μ_{unc} because the magnetization curve at $T > T_B$ is described by the Langevin function the expansion in series of which yields a linear dependence $\chi(\mu_{unc}) \sim \mu_{unc}/kT$ and leads eventually to the relation $\chi \sim V^{1/2}$. At the same time, it follows from relation (1) that $T_B \sim V$. However, these relations do not take into account fac-

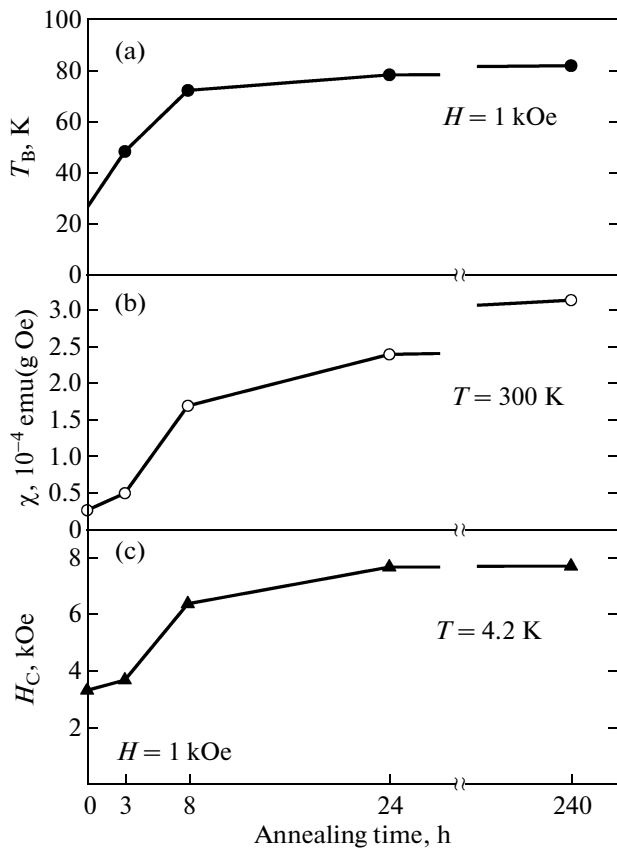


Fig. 3. Plots of (a) blocking temperature T_B , (b) magnetic susceptibility χ at $T = 300$ K, and (c) coercivity H_C at $T = 4.2$ K vs. low-temperature annealing time.

tors such as the particle size distribution, surface phenomena (in which the magnetic anisotropy constant K also depends on the particle size). Nevertheless, the values of T_B , H_C , and χ are proportional to the particle size.

Figure 3 summarizes data on the variation of T_B , H_C , and $\chi(T = 300$ K) with the duration of low-temperature heat treatment. As can be seen, all these parameters exhibit several-fold growth after 240-h annealing and the most rapid variation of T_B , H_C , and χ takes place for treatment durations below 24 h. Therefore, it may be concluded that annealing leads to an increase in particle dimensions, which is probably related to the agglomeration of closely spaced particles.

Figure 2 presents some data on the properties of annealed ferrihydrite exposed in saturated water vapor: $\chi(T)$ of sample FH-24-H (curve 4) and $M(H)$ of the sample FH-240-H (inset). Note that these values almost coincide with those for the corresponding samples upon annealing, provided that the susceptibility and magnetic moment are multiplied by a coefficient

that takes into account an increase in the sample mass. The values of T_B and H_C also remain almost unchanged. Although analysis of Mössbauer spectra reveals some changes in the local environment of iron atoms, the magnetic data lead to the conclusion that particle dimensions do not change as a result of exposure in saturated water vapor.

Analysis of data on small-angle X-ray scattering in ferrihydrite samples analogous to the initial sol (FH-0) showed that these particles have a characteristic size of several nanometers [12], which corresponds to ~ 2000 – 2500 iron atoms per particle [6]. The results of our investigation lead to the conclusion that heat treatment at relatively low temperature (150°C) for 24–240 h results in a several-fold growth in the average volume of particles (and about twofold increase in their average linear size), which is accompanied by an increase in H_C ($T = 4.2$ K), T_B , and χ ($T = 300$ K). A controlled increase in the room-temperature magnetic susceptibility of nanoparticles at an average size of ~ 10 nm can be of practical significance, since this value directly determines the driving force that acts on the particles occurring in a liquid medium. Thus, ferrihydrite nanoparticles exposed in an aqueous medium are stable and their integral magnetic properties remain unchanged.

Acknowledgments. This study was supported in part by the Ministry of Education and Science of the Russian Federation in the framework of a federal program for 2014–2016.

REFERENCES

1. N. J. O. Silva, V. S. Amaral, and L. D. Carlos, *Phys. Rev. B* **71**, 184408 (2005).
2. V. F. Babanin, Yu. M. Gorovoi, A. A. Zalutskii, P. A. Ivanov, and A. V. Morozov, *Tech. Phys. Lett.* **38** (3), 238 (2012).
3. Yu. L. Raikher and V. I. Stepanov, *J. Exp. Theor. Phys.* **107** (3), 435 (2008).
4. S. Morup, D. E. Madsen, C. Fradsen, C. R. H. Bahl, and M. F. Hansen, *J. Phys.: Condens. Matter* **19**, 213202 (2007).
5. Yu. L. Raikher, V. I. Stepanov, S. V. Stolyar, V. P. Ladygina, D. A. Balaev, L. A. Ishchenko, and M. Balasoiu, *Phys. Solid State* **52** (2), 298 (2010).
6. D. A. Balaev, A. A. Dubrovskii, A. A. Krasikov, S. V. Stolyar, R. S. Iskhakov, V. P. Ladygina, and E. D. Khilazheva, *JETP Lett.* **98** (3), 135 (2013).
7. D. A. Balaev, A. A. Krasikov, A. A. Dubrovskii, S. V. Semenov, O. A. Bayukov, S. V. Stolyar, R. S. Iskhakov, V. P. Ladygina, and L. A. Ishchenko, *J. Exp. Theor. Phys.* **119** (3), 479 (2014).

8. S. V. Stolyar, O. A. Bayukov, Yu. L. Gurevich, E. A. Denisova, R. S. Iskhakov, V. P. Ladygina, A. P. Puzyr', P. P. Pustoshilov, and M. A. Bitekhtina, *Inorg. Mater.* **42** (7), 763 (2006).
9. S. V. Stolyar, O. A. Bayukov, Yu. L. Gurevich, V. P. Ladygina, R. S. Iskhakov, and P. P. Pustoshilov, *Inorg. Mater.* **43** (6), 638 (2007).
10. S. V. Stolyar, O. A. Bayukov, V. P. Ladygina, R. S. Iskhakov, L. A. Ishchenko, V. Yu. Yakovchuk, K. G. Dobretsov, A. I. Pozdnyakov, and O. E. Piksina, *Phys. Solid State* **53** (1), 100 (2011).
11. E. Stoner, *Phil. Trans. Roy. Soc. (London), Ser. A* **240**, 599 (1948),
12. M. Balasoiu, S. V. Stolyar, R. S. Iskhakov, L. A. Ischenko, Y. L. Raikher, A. I. Kuklin, O. L. Orelovich, Yu. S. Kovalev, and T. S. Kurkin, *Rom. J. Phys.* **55** (7–8), 782 (2010).

Translated by P. Pozdeev